EUROPEAN ORGANIZATION FOR NUCLEAR RESEARCH

CERN-EP/86-36
20 March 1986

A MODULAR MUTLIDRIFT VERTEX DETECTOR

R. Bouclier, G. Charpak, W. Gao*), Ph. Miné**), A. Peisert, J.C. Santiard,
F. Sauli and N. Solomey***)

CERN, Geneva, Switzerland

ABSTRACT

We have built and tested several 80 cm long multiwire drift tubes, each with 128 independent drift cells consisting of individual anodes centred in a hexagonal cell, 1 mm in radius, defined by six cathode wires. A thin hexagonal carbon-fibre envelope supports the wire tension and provides gas tightness. Charged tracks are measured recording drift times on all anodes, on an average ten times on each module; the longitudinal coordinate can be measured from current division at the two ends of each wire. Several modules can be packed to build a compact, fast vertex detector suitable for collider experiments.

To appear in the
Proceedings of the Wire Chamber Conference,
25–28 February 1986

---

*) On leave from the Institute of High-Energy Physics, Beijing, People's Republic of China.
**) Permanent address: Ecole Polytechnique, Paris, France.
***) Permanent address: Ohio State University, Columbus, Ohio, USA.

The most difficult region to instrument in a detector for collider experiments is the central one, close to the vacuum tubes, where the density of tracks and the background rate are the largest. This is moreover the most inaccessible region of the set-up; a major breakdown there has the worst consequences for the whole operation. Solid-state devices are being developed to fulfil these experimental needs, but at the present time they are still too expensive to allow the implementation of more than a few sensitive layers; there are also serious concerns about the mass and the radiation resistance of such detectors in a high-rate environment. A gaseous multiwire detector, providing many measured points in a relative thin layer, is still the only practical way to obtain good tracking close to the interaction point. A limitation in the use of multiwire proportional chambers lies, however, in their relative fragility, especially if subjected to accidental breakdown, because of the use of thin wires. One way of improving the reliability of a system based on gaseous wire detectors is to increase its modularity and redundancy; such an approach was originally taken by a group at SLAC with the development of cheap, mass-produced individual drift tubes or straws that can be assembled together to constitute a complete detector [1]. Extending this concept further, we have built several multidrift modules having many independent drift cells packed within a thin carbon-fibre supporting tube, of hexagonal shape, that constitutes also the gas envelope [2, 3]. Each sensitive cell consists of an anode wire centred in a hexagonal drift structure, 1 mm in radius, with cathode wires at the corners; our first prototypes had 128 anodes per module. Many tubes can be closely packed, for example in a cylindrical geometry, to instrument the central region in a collider detector; in the case of failure, individual modules may be disconnected or replaced. A contact with the anode wires is available at both ends of the module, to allow determination of the longitudinal coordinate through a measurement of the current ratio on the resistive wire.

To analyse the resolution properties of the device and optimize the pattern recognition, we have developed a detailed Monte Carlo event generation program that takes into account the primary and total ionization statistics as well as the electron drift and diffusion in the cells of the detector. The simulation indicates that an average reconstruction accuracy of 100 μm r.m.s. should be achievable on each cell; in the complete tube, a single track is measured on an average a dozen times with the quoted accuracy. For two close tracks only the coordinate nearest to each wire is measured; the geometry is such, however, that on an average each track will still be recorded on alternate wires and can be reconstructed, although on a reduced number of wires. We expect indeed a two-track resolution of several hundred microns, somewhat depending on the sophistication of the software reconstruction algorithm. For dense concentrations of tracks, as in jets or for calorimetry applications, the envelope of the cluster of tracks should still be well determined.

The principle of construction of a module can be described using figs. 1 and 2. Wires are strung between two high-quality fibre-glass plates*) of hexagonal shape, 4 mm thick and 30 mm in diameter, through a set of holes 600 μm in diameter drilled on a high-precision numerical boring machine. A 50 μm thick copper sheet is glued on one side of the plate before drilling; all pins holding the cathode wires, once inserted and kept under tension, make contact with this common electrode that distributes the high voltage. As can be seen in the figures, a short, larger diameter (1.2 mm) bore around the holes destined to receive the anodes ensures the insulation of these pins from the cathodes. Wires are soldered to metal pins inserted in the holes of the supporting plates; these pins are precision-machined brass cylinders**), 0.8 mm in diameter, reducing to 0.6 mm at the tip, in the section inserted into the plate. A V-shaped groove, cut over

*) Made by Stesalit AG, Zullwil, Switzerland.

**) Manufactured by DECSO, Moutier, Switzerland.

the full length of the cylinder, receives the wire before soldering. Because of the different diameters of the corresponding wires, anode and cathode pins have grooves with a different depth to ensure proper centring; the cathode pins are also shorter, and are completely covered by epoxy in the last phase of manufacturing. The central bore receives a stainless-steel tube, in contact with the copper layer, that will serve both as gas and high-voltage inlet. We have used 25 μm diameter gold-plated tungsten for the anodes and 70 μm copper–beryllium wires for cathodes, tensioned at 60 and 120 g, respectively.

To assemble the module, the two end-plates are inserted on temporary brackets, rigidly mounted on a connecting horizontal bar. Wires are individually pulled through facing holes in the end plates, and kept under tension by a system of pulley and sprocket. The appropriate brass pins are inserted on each side, with the wire resting in the grooves face-up; wires are then soldered with a low-melting-point alloy and cut at both ends. The assembly proceeds in layers, starting from the lowest; fig. 3 shows one of the end plates after completion of the wiring. The insulation between wires and their mechanical strength are verified repeatedly during assembly, applying a high voltage to the common cathodes and grounding the anodes through a very-high-value resistor and a current meter. Defective wires can be easily spotted and replaced at this stage of construction. Once the wiring is completed, the fibre-glass plates are fastened to a coaxial support fixed to three threaded pins on the corners, insulated from the copper layer (they will be used later to fasten the connector); on one side, the support consists of a long rod on which the supporting tube has been previously inserted, as shown in fig. 3. The carbon-fibre tube used for the prototypes is 80 cm long and 550 μm thick, with an outer diameter of 32 mm; it is composed of carbon and epoxy in almost equal proportions*). The temporary brackets are then removed, all wires being kept under tension by the coaxial mounting, and the carbon-fibre tube is slid over the wires to its final position. The whole supporting bar is turned by 90° and epoxy is poured over the top plate thus both sealing the tube to the plate and covering all cathode pins. After curing, the same procedure is repeated on the opposite plate, turning over the assembly. The module is now ready for testing. Figure 4 shows a close view of one end of a completed module: one can recognize the top of the anode pins, the central tube that provides both the gas inlet and the high-voltage connection, and the three threads used for fastening the signal connector.

As mentioned above, all anode wires (128 on each module) can be read out on both sides of the tube; for the measurements described here, however, we have only recorded the drift time on all wires from one side, using a system of discrete electronics elements connected to the anodes with short (50 cm) miniature coaxial cables. Because of the high density of output contacts, we had to develop a specialized connector to bring the signals to the electronics board. After several attempts using various kinds of mechanical spring-loaded and conductive pad contacts, which had rather poor reliability, we have adopted the solution sketched in fig. 2. It consists of an anisotropic conducting membrane inserted between the anode pins and the printer-circuit matrix to which the cables are soldered. The membrane is a thin (0.3 mm) rubbery sheet with thousands of short metal wires, perpendicular to the surface, and insulated from each other**). With our contact surface (0.5 mm^2) the serial resistivity is typically 2–3 Ω; the insulation between adjacent contacts is above 100 MΩ.

---

*) Manufactured by Compagnie francaise des isolants, Crépy-en-Valois, France.

**) Made by Shin-Etsu Polymer Co, Shin-Etsu Bld, Tokyo, Japan.

We have used for detection a fast amplifier–discriminator circuit, developed at CERN [4] and manufactured in thick-film hybrid form*). With a charge-discrimination threshold that can be regulated from 10^{-2} pC up and 3 ns time slewing for a 40 dB variation in the input signal, the circuit allows precise drift-time measurements. The shaped output from the discriminators is sent to logical receivers in the counting room via flat twisted-pair cables, and the drift time measured with multichannel time-to-digital converters set at 10 channels per nanosecond sensitivity. For the beam tests, the time reference was provided by a scintillation-counter coincidence. Data were recorded with a small on-line computer, and analysed off-line.

The first measurements realized with a full prototype confirmed the relative ease of operating the counter in many gas mixtures; to limit the dangers of edge discharges inside the supporting plate and of electrostatic instabilities we preferred, however, to use relatively small fractions of quenchers in order to limit the absolute working voltage. We have tested various mixtures of argon and xenon with isobutane, ethane, methylal, and freon, all at atmospheric pressure. Because of the small size of the drift cell, we expect the localization accuracy to be dominated by the primary ionization statistics; the best results are obtained in this case if one is able to detect the first electron reaching the wire. For this reason we have used for part of the tests the so-called magic gas that allows very large and saturated gains: a mixture of argon (74.5%) + isobutane (21%) + methylal (4%) + freon (CF_3Br) (0.5%); the addition of methylal helps to reduce the ageing problems at high rates [5]. A measurement of average pulse heights recorded in this gas on a single wire in the module, both for minimum ionizing electrons and 5.9 keV X-rays, is given in fig. 5; at the highest operational voltage, the two curves tend to converge as expected because of gain saturation. Figure 6 shows the efficiency plateau measured in the same condition for minimum ionizing electrons on the fully instrumented tube and a discrimination threshold on each wire of 3×10^{-2} pC. For the beam tests, data were recorded at several values of high voltage within the region of full efficiency; a single-electron efficiency is obtained, however, only at the highest values.

The origin of the measured coordinate for each channel, or time zero, is deduced from the data histogramming the drift-time spectra for individual wires; after subtraction of this quantity and multiplication by a slope constant (also specific for each channel and determined from a previous electronic calibration), we obtain the drift time as measured event per event by the hit wires. A first approximation of the distances between tracks and wires is then obtained by multiplying the measured time by a constant drift velocity (4.4 cm/μs in the magic gas).

While most of the events recorded in the test are straight beam tracks, some (probably due to electron shower) have a rather complex geometry; an example that illustrates the good imaging capability of the module is given in fig. 7. Circles around the hit wires represent the measured drift time; for the time being, tracking has not been attempted for this kind of event.

Data are unfortunately not available to allow computing of the space–time correlation in the very large range of fields across a cell in our gases; we expect indeed the drift velocity to increase in the high field close to the anode wire. This is obviously a very critical point, and we plan in the near future to measure the correlation directly using a collimated UV laser.

The off-line straight track finding proceeds then as follows. A first-level linear fit is attempted using only the hit-wire location (disregarding the actual value of the drift time). On the perpendicular to the fitted track from the hit wires, the shorter distance is selected using the drift-time measurement (this solves the right–left ambiguity intrinsic in the detector); points

---

*) Type NMC842, manufactured by Newmarket Microsystems Ltd., Exning Road, Newmarket, Suffolk, United Kingdom.

having a distance from the initial track exceeding a given tolerance (2 mm) are discarded as background. The fit is then repeated with the new set of coordinates and a difference Δ between the measured and the fitted distance is calculated for every point. We then reject points with $\Delta > 350$ μm and $\Delta < -250$ μm. This asymmetry reflects the fact that the measured distance can be bigger than the real one owing to finite distance between primary collisions (about 250 μm in our conditions) but cannot be smaller. This procedure converges rapidly for single tracks accompanied eventually by single-hit background. However, it does not resolve double tracks or single tracks accompanied by a cluster of discharging wires. Figure 8 shows both the average and spread (r.m.s.) of the residuals Δ as a function of the fitted track distance to the wire (black dots with error bars). One can see that the measured coordinates are systematically larger than the fitted ones for short drift distances owing to the dominant effect of the primary ionization statistics for tracks close to the wire.

We have reproduced this purely statistical effect well with a Monte Carlo simulation, as shown in the figure (open dots). Although of course there is no way of removing this source of error, one should probably include in the fit procedure a weighting function that takes into account the asymmetry in the errors for close tracks. For the time being this has not been done, and one should retain an average measurement error for each point of 100 μm r.m.s., almost independent of the drift distance. For every event we calculate the average single-wire resolution σ from

$$\sigma^2 = \Sigma(r_{meas} - r_{fitted})^2/(N - 2),$$

where r_{meas} and r_{fitted} are measured and fitted track distances to the wire, and N is the number of points used in the fit. Because of the systematic displacements in the distribution of the residuals, we obtain so far a rather coarse resolution with a r.m.s. of 140 μm, which has to be considered the average reconstruction accuracy for a single wire at the present state of the analysis.

If after the first rejection of distant points the resolution exceeds a given value (750 μm) the program separates all points into two sets according to their side with respect to the fitted line. These two sets are then input to the fitting routine. An example of a reconstructed double-track event is given in fig. 9; circles around the wires represent the measured distance from hit wires, as given by the drift time using the above-mentioned phenomenological space–time correlation, and the straight lines are the result of the fit.

The success of this approach to the realization of a high-rate, high-resolution detector will depend, of course, on the finding of cheap and reliable construction techniques, as well as the development of high-density electronics.

Apart from its use as vertex detector in elementary particle physics, the modular approach can be foreseen to be of interest in other fields of research where reliability is a major concern. With a xenon gas filling, a stack of multidrift tubes seems appropriate for a parallax-free, high-rate detection of soft X-rays for various biomedical applications.

REFERENCES

[1] D. Rust, SLAC-PUB-3311 (1984).

[2] R. Bouclier, G. Charpak and F. Sauli, CERN EP Int. Rep. 84-03 (1984).

[3] R. Bouclier, G. Charpak, L. Ropelewski, J.C. Santiard, N. Solomey and F. Sauli, submitted to IEEE Nuclear Science Symposium, San Francisco, October 1985.

[4] J.C. Santiard, A low threshold hybrid amplifier-discriminator, CERN EP Int. Rep. 82-04 (1982).

[5] G. Charpak, H.G. Fisher, C.R. Gruhn, A. Minten, F. Sauli, G. Plch and G. Flügge, Nucl. Instrum. Methods **99** (1972) 279.

Figure captions

Fig. 1 : Schematics of the drilling geometry of the end plates. Small circles represent holes for inserting the wire-holding pins; around the anodes, a short, larger-diameter drill ensures insulation against the metallized surface of the plate.

Fig. 2 : Cross-section of the end-plate assembly. Once inserted and wired, cathode pins are completely embedded in epoxy, the common contact being provided by a central tube (not shown) through the copperized upper layer of the plate. The system of signal connection, which makes use of an anisotropic conducting sheath, is also shown.

Fig. 3 : View of the wired multidrift module before final assembly. The carbon-fibre tube, to be inserted over the plates after removal of the temporary support, is also visible.

Fig. 4 : One end of a finished module. Contacts with the anode pins are visible, as well as the central tube for the gas- and high-voltage supply. The three threaded pins are used for assembly and to hold the signal connector in place.

Fig. 5 : Average pulse height for minimum ionizing electrons and 5.9 keV X-rays, as a function of voltage. The gain saturation typical of the magic-gas operation is apparent.

Fig. 6 : Efficiency plateau for minimum ionizing electrons, measured in a fully instrumented module with magic-gas filling.

Fig. 7 : Example of on-line display of a complex event. The circles represent the measured drift-time on the hit wires.

Fig. 8 : Difference of measured and fitted points as a function of the fitted track distance. Black dots with error bars represent the experimental points, open dots are simulated.

Fig. 9 : An example of a double-track event, fitted by the reconstruction program. One can observe some inefficiency in the tube, due to the operation at a lower voltage than usual for this particular measurement.

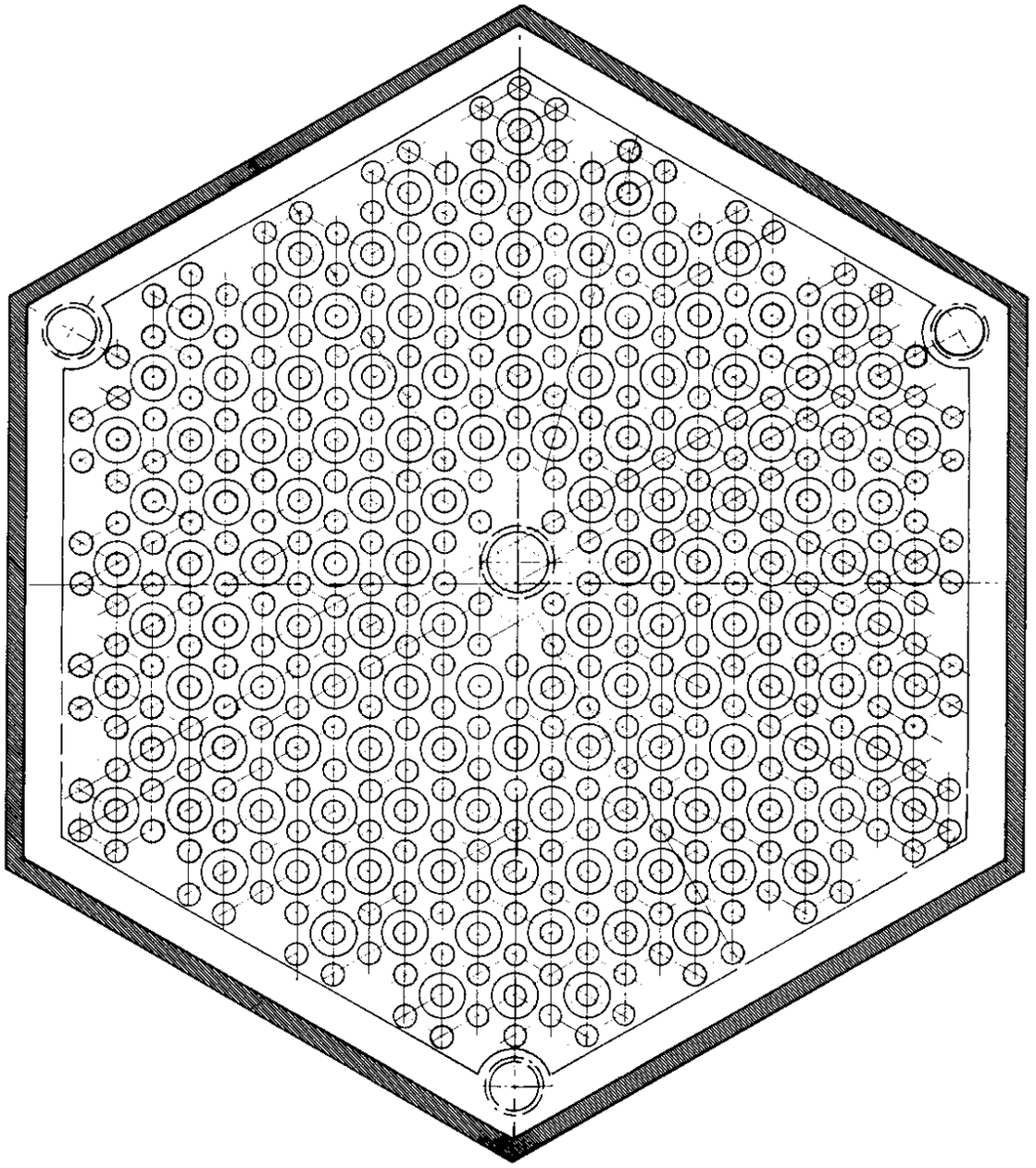

Fig. 1

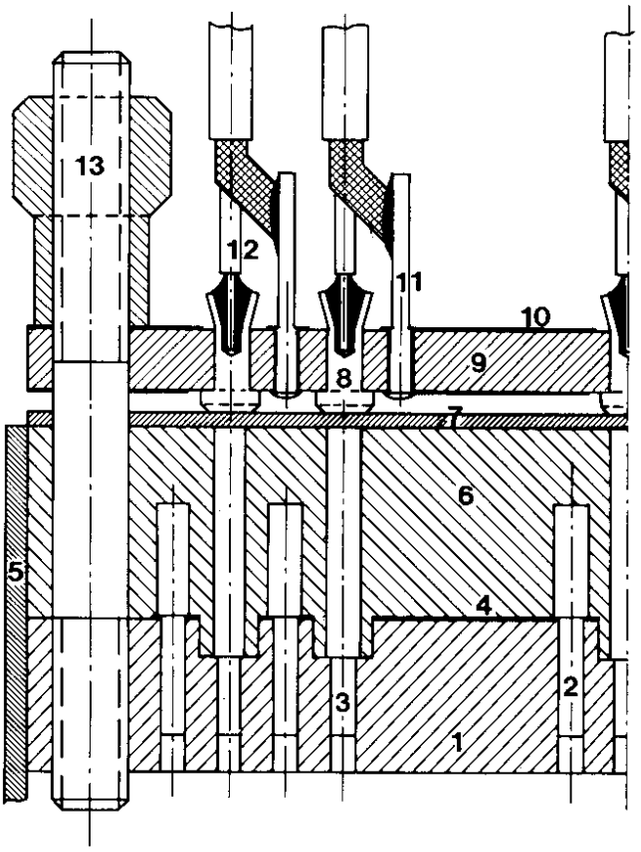

1: Main fibre-glass end plate
2: Cathode-wire pin
3: Anode-wire pin
4: Copper layer for HV connection
5: Carbon-fibre tube
6: Epoxy insulating layer
7: Soft conductive rubber
8: Rivets
9: Printed circuit
10: Ground connection
11: Soldering lugs
12: Signal cable
13: Fastening pins

Fig. 2

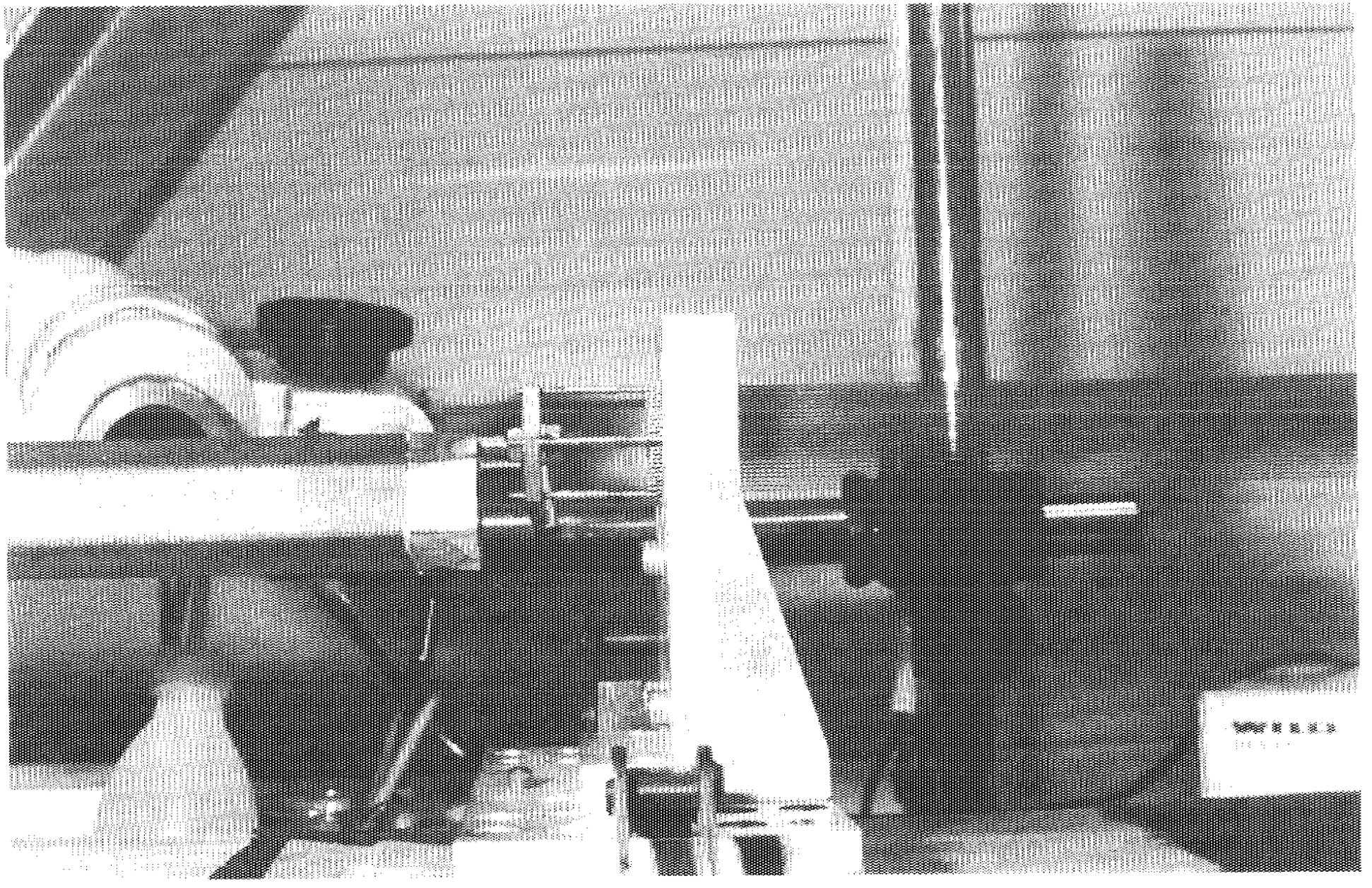

Fig. 3

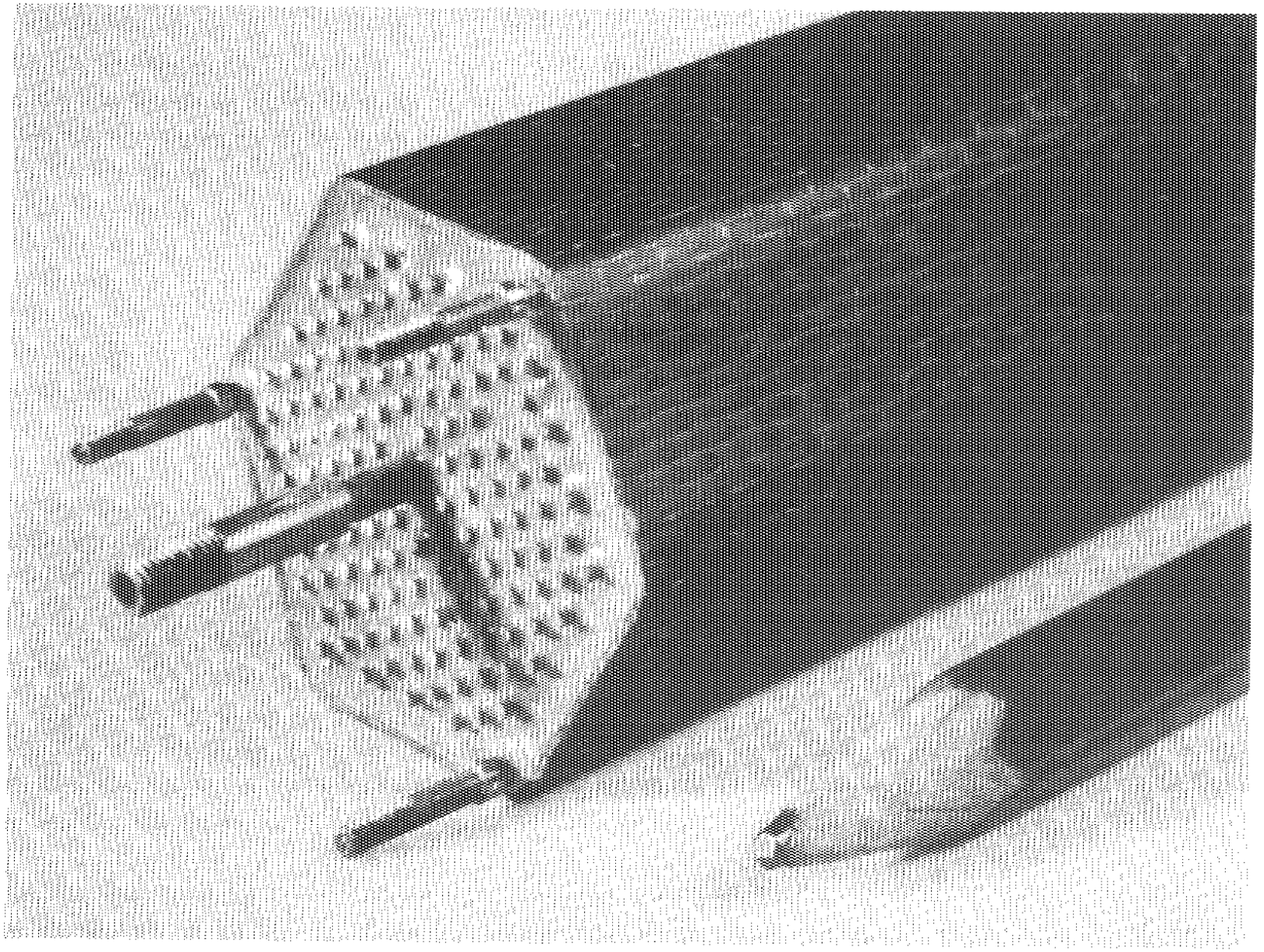

Fig. 4

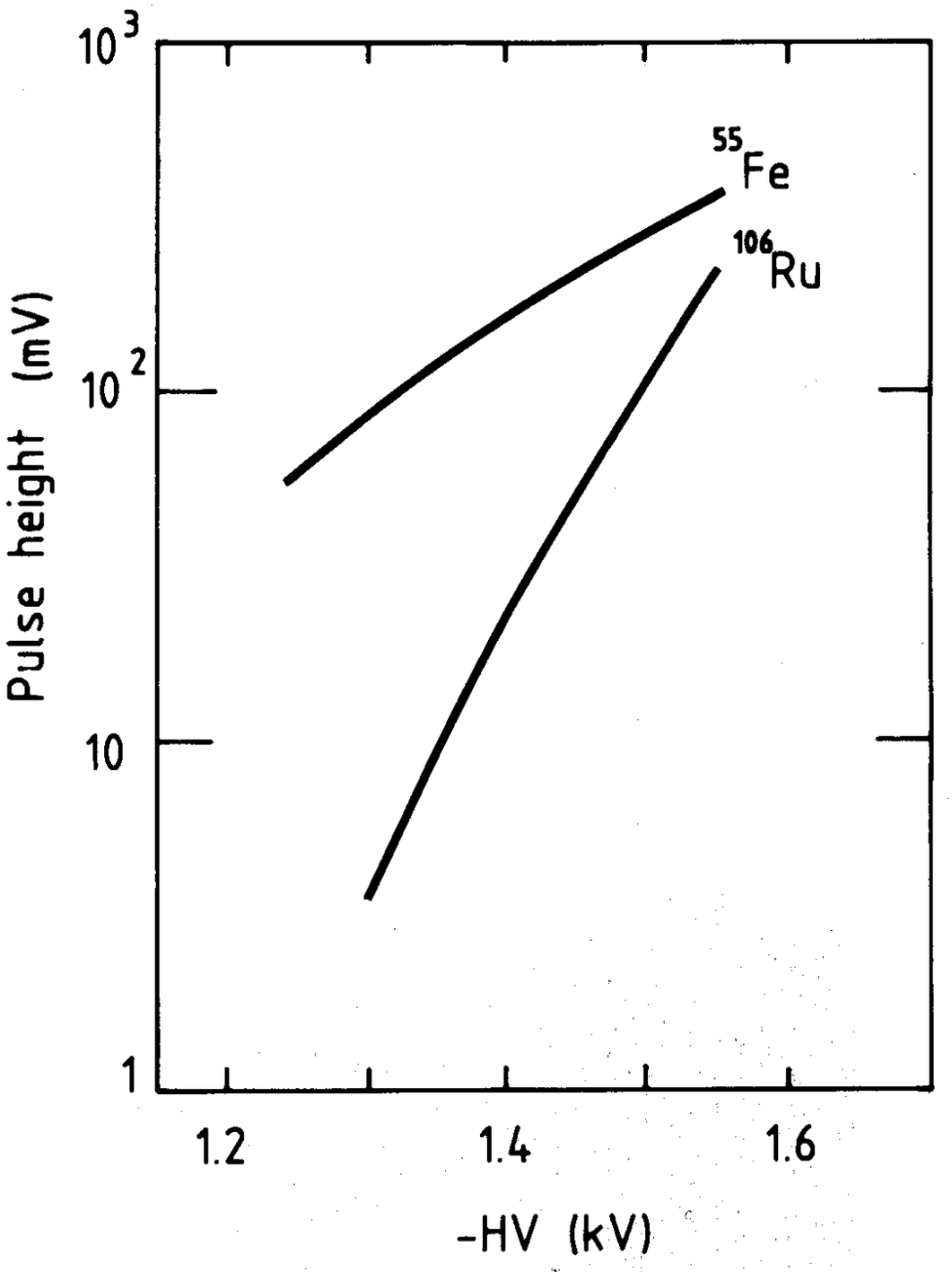

Fig. 5

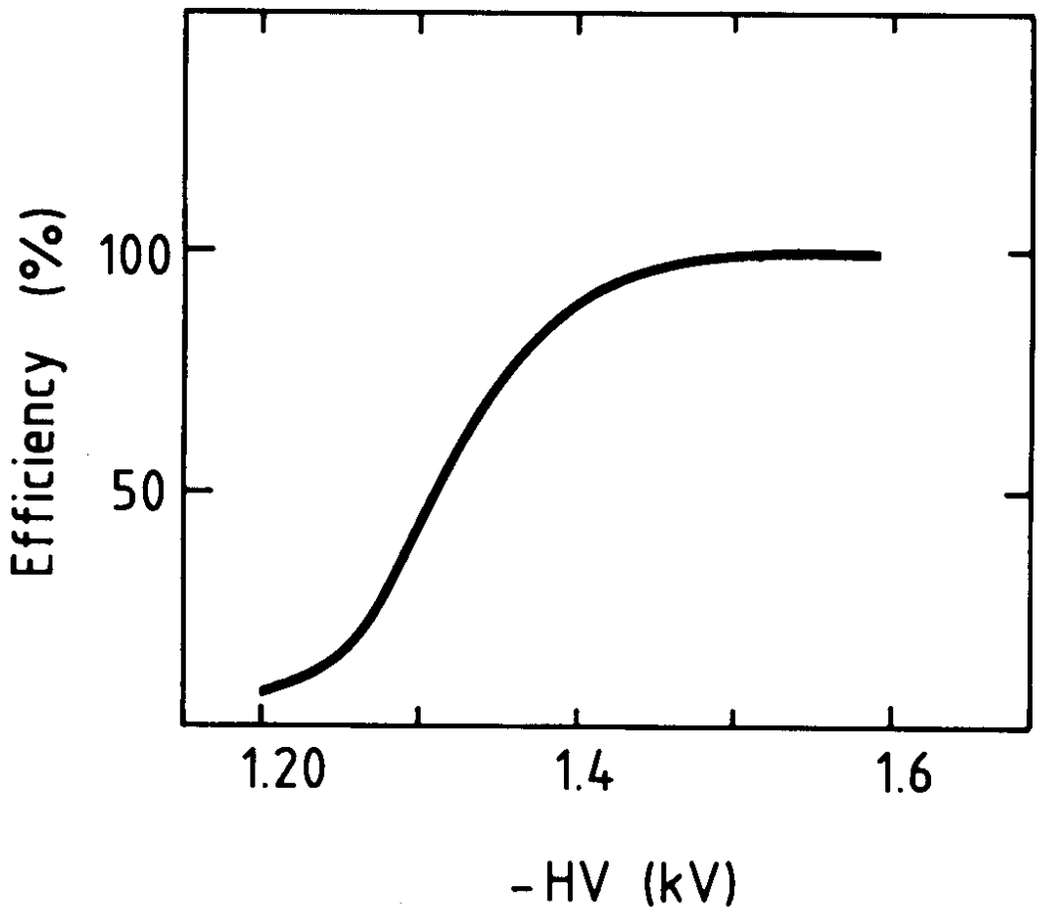

Fig. 6

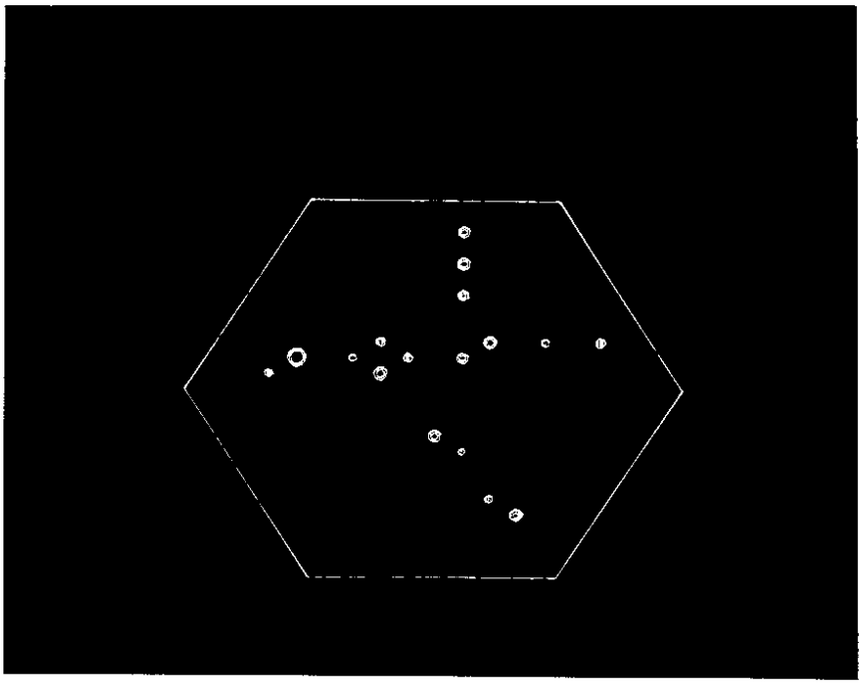

Fig. 7

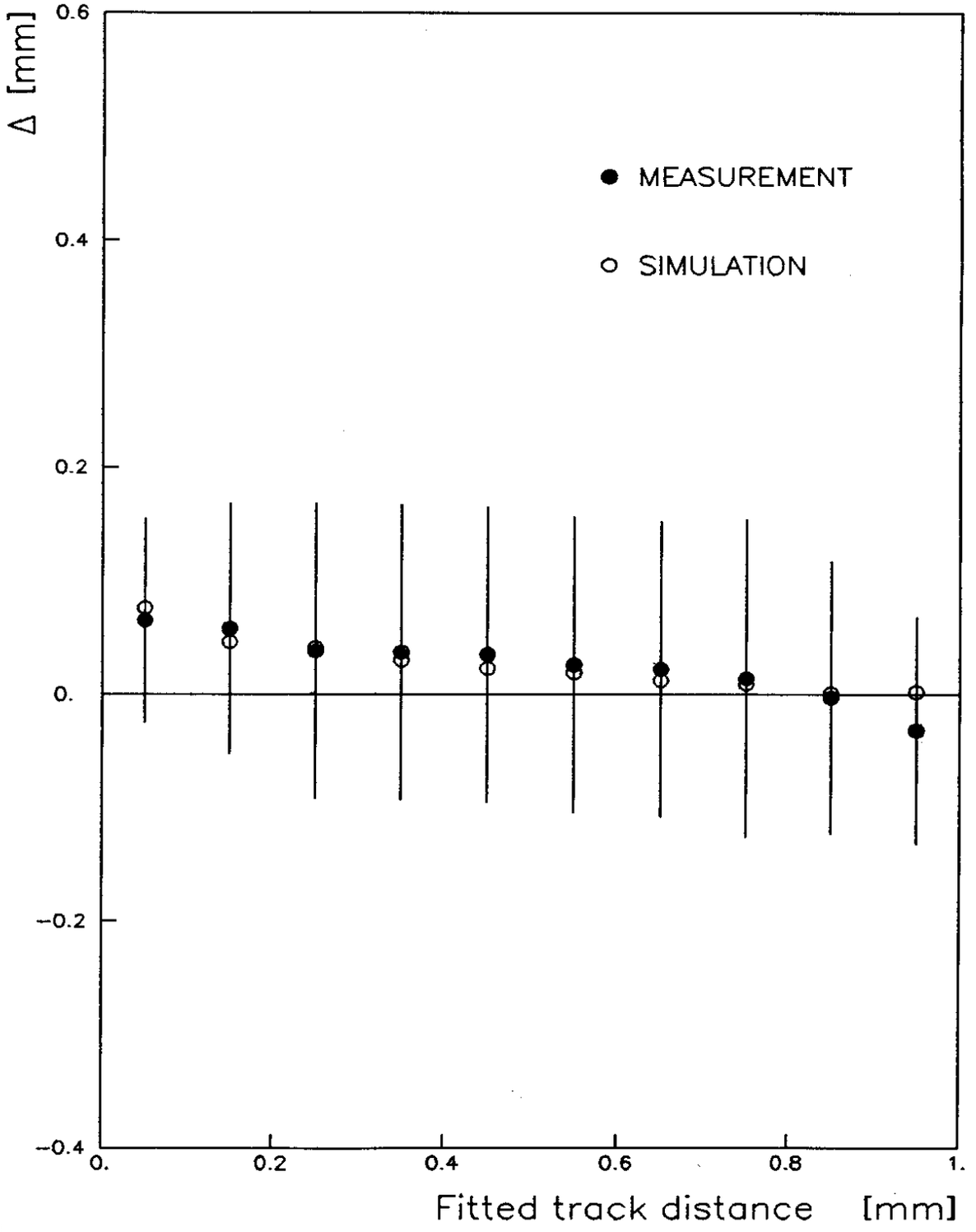
Δ [mm]
0.6
0.4
0.2
0.
−0.2
−0.4
MEASUREMENT
SIMULATION
0.
0.2
0.4
0.6
0.8
1.
Fitted track distance [mm]

Fig. 8

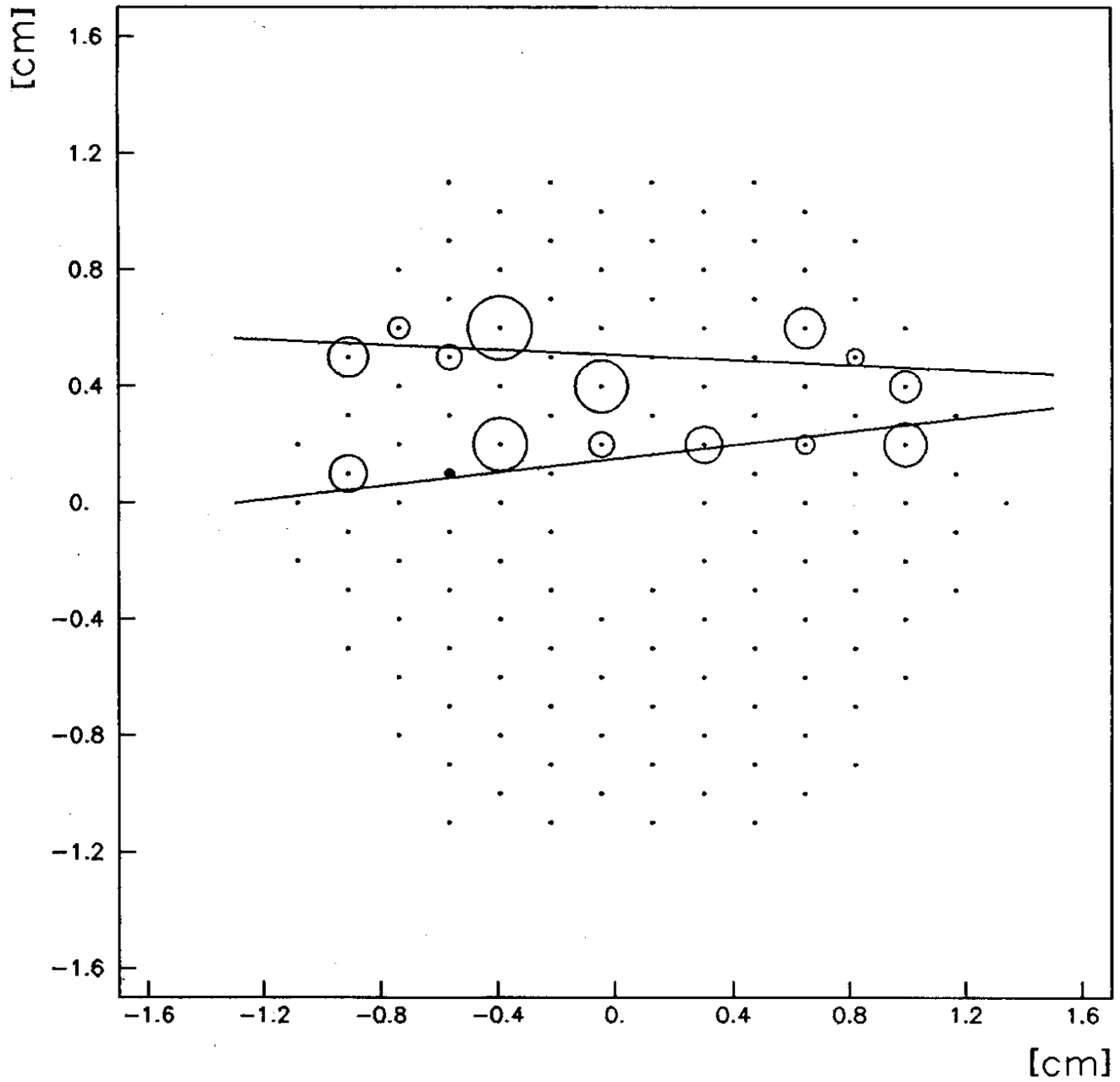

Fig. 9